Review

JOURNAL OF COMPOSITE MATERIALS

Journal of Composite Materials
2022, Vol. 56(23) 3635–3649

DOI: 10.1177/00219983221116432
journals.sagepub.com/home/jcm
SAGE

Extraordinary disordered hyperuniform multifunctional composites

Salvatore Torquato

Abstract

A variety of performance demands are being placed on material systems, including desirable mechanical, thermal, electrical, optical, acoustic and flow properties. The purpose of the present article is to review the emerging field of disordered hyperuniform composites and their novel multifunctional characteristics. Disordered hyperuniform media are exotic amorphous states of matter that are characterized by an anomalous suppression of large-scale volume-fraction fluctuations compared to those in "garden-variety" disordered materials. Such unusual composites can have advantages over their periodic counterparts, such as unique or nearly optimal, direction-independent physical properties and robustness against defects. It will be shown that disordered hyperuniform composites and porous media can be endowed with a broad spectrum of extraordinary physical properties, including photonic, phononic, transport, chemical and mechanical characteristics that are only beginning to be discovered.

Keywords

disordered composites, hyperuniformity, multifunctionality

Introduction

Increasingly, a variety of performance demands are being placed on material systems. In aerospace and space applications these requirements include lightweight component structures that have desirable mechanical, thermal, electrical, optical, acoustic and flow properties. Structural components should be able to carry mechanical loads while having other beneficial performance characteristics. Desirable thermal properties include high thermal conductivity to dissipate heat and thermal expansion characteristics that match the attached components. In the case of porous cellular solids, heat dissipation can be improved by forced convection through the material, but in these instances the fluid permeability of the porous material must be large enough to minimize power requirements for convection. Desirable optical and acoustic properties include materials that can control the propagation of light and sound waves through them. It is difficult to find single homogeneous materials that possess these multifunctional characteristics.

By contrast, composite materials are ideally suited to achieve multifunctionality, since the best features of different materials can be combined to form a new material that has a broad spectrum of desired properties.[1–5] These materials may simultaneously perform as ultralight load-bearing structures, enable thermal and/or electrical management, ameliorate crash or blast damage, and have desirable optical and acoustic characteristics. A general goal is the design of composite materials with N different effective properties or responses, which we denote by $K_e^{(1)}, K_e^{(2)}, \ldots, K_e^{(N)}$, given the individual properties of the phases. In principle, one desires to know the region (set) in the multidimensional space of effective properties in which all composites must lie (see Figure 1 for a two-dimensional (2D) illustration). The size and shape of this region depends on the prescribed phase properties as well as how much microstructural information is specified, For example, the set of composites with unspecified volume fractions is clearly larger than the set in which the the volume fractions are specified.

The determination of the allowable region is generally a highly complex problem. Cross-property bounds[3,6–16] can aid to identify the boundary of the allowable region and numerical topology optimization methods[17–21] can then be used to find specific microstructures that lie on the boundary, which are extremal solutions. These methods often bias the solutions to be periodic structures with high

Princeton University, Princeton, NJ, USA

Corresponding author:
Salvatore Torquato, Department of Chemistry, Department of Physics, Princeton Institute of Materials, and Program in Applied and Computational Mathematics, Princeton University, Frick Lab, Princeton, NJ 08544, USA
Email: torquato@princeton.edu

crystallographic symmetries. As we will see below, it can be very beneficial to constrain the optimal solution set to microstructures possessing "correlated disorder",[22] which can have advantages over periodic media, especially an exotic type of disorder within the so-called hyperuniformity class.[23,24] The purpose of the present article is to review the emerging field of disordered hyperuniform composites and their novel multifunctional characteristics.

The hyperuniformity concept was introduced and studied nearly two decades ago in the context of many-particle systems.[23] Hyperuniform systems are characterized by an anomalous suppression of large-scale density fluctuations compared to "garden-variety" disordered systems. The hyperuniformity concept generalizes the traditional notion of long-range order in many-particle systems to not only include all perfect crystals and perfect quasicrystals, but also exotic amorphous states of matter. Disordered hyperuniform materials can have advantages over crystalline ones, such as unique or nearly optimal, direction-independent physical properties and robustness against defects.[16,22,25–42]

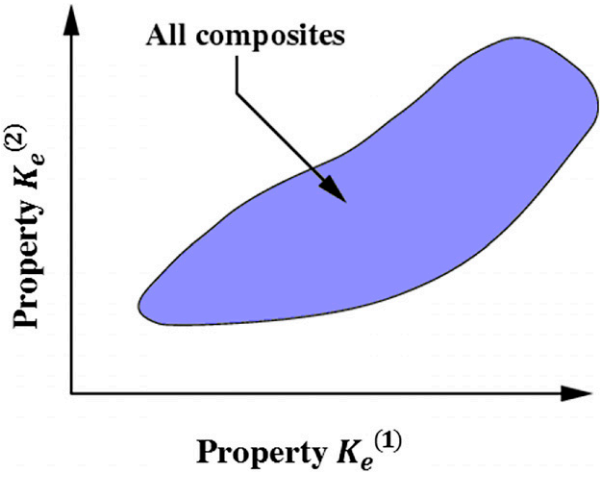

Figure 1. Schematic illustrating the allowable region in which all composites with specified phase properties must lie for the case of two different effective properties, $K_e^{(1)}$ and $K_e^{(2)}$, as adapted from Ref. 19. Importantly, this allowable region depends on the type of microstructural information that is specified.

The hyperuniformity concept was generalized to two-phase heterogeneous media in d-dimensional Euclidean space $\mathbb{R}^d$,[24,43] which include composites, cellular solids and porous media. A two-phase medium in $\mathbb{R}^d$ is hyperuniform if its local volume-fraction variance $\sigma_V^2(R)$ associated with a spherical observation window of radius R decays in the large-R limit faster than the inverse of the window volume, i.e., $1/R^d$; (see Structural characterization of disordered hyperuniform composites for mathematical details). This behavior is to be contrasted with those of "typical" disordered two-phase media for which the variance decays like the inverse of the window volume (see Figure 2).

In this article, we review progress that has been made to generate and characterize multifunctional disordered two-phase composites and porous media. In Structural characterization of disordered hyperuniform composites, we collect basic definitions and background on hyperuniform and nonhyperuniform two-phase media. In Forward approaches to generating disordered hyperuniform two-phase media and Inverse approaches to generating disordered hyperuniform two-phase media, we review developments in generating disordered hyperuniform two-phase media using forward and inverse approaches, respectively. In Order metrics for disordered hyperuniform two-phase media, we describe order metrics that enable a rank ordering of disordered hyperuniform two-phase media. In Novel multifunctional disordered hyperuniform composites and porous media, we review the current knowledge about the extraordinary multifunctional characteristics of disordered hyperuniform composites and porous media. Finally, In Conclusions and outlook, we make concluding remarks and

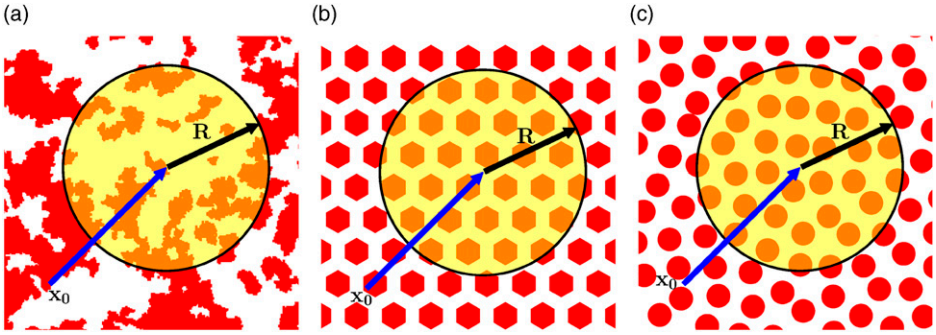

Figure 2. Schematics indicating a circular observation window of radius R in two dimensions and its centroid $\mathbf{x}_0$ for a "typical" disordered nonhyperuniform (a), periodic (b), and disordered hyperuniform (c) media. In each of these examples, the phase volume fraction within the window will fluctuate as the window position varies. Whereas the local variance $\sigma_V^2(R)$ for the nonhyperuniform medium decays like $1/R^2$ for large R, it decays like $1/R^3$ in both the periodic and disordered hyperuniform examples. In space dimension d and for large R, $\sigma_V^2(R)$ scales like $1/R^d$ and $1/R^{d+1}$ for nonhyperuniform and hyperuniform media, respectively.

discuss the outlook for the field.

Structural characterization of disordered hyperuniform composites

For two-phase heterogeneous media in d-dimensional Euclidean space $\mathbb{R}^d$, hyperuniformity can be defined by the following infinite-wavelength condition on the *spectral density* $\tilde{\chi}_V(\mathbf{k})$,[24,43] i.e.

$$\lim_{|\mathbf{k}|\to 0} \tilde{\chi}_V(\mathbf{k}) = 0 \tag{1}$$

where $\mathbf{k}$ is the wavevector. The spectral density $\tilde{\chi}_V(\mathbf{k})$ is the Fourier transform of the autocovariance function $\chi_V(\mathbf{r}) \equiv S_2^{(i)}(\mathbf{r}) - \phi_i^2$, where ϕ_i is the volume fraction of phase i, and $S_2^{(i)}(\mathbf{r})$ gives the probability of finding two points separated by $\mathbf{r}$ in phase i at the same time.[3] This two-point descriptor in Fourier space can be easily obtained for general microstructures either theoretically, computationally, or via scattering experiments.[44] The distinctions between the spectral densities for examples of 2D hyperuniform and nonhyperuniform media can be vividly seen in the top panel of Figure 3.

Hyperuniformity of two-phase media can be also defined in terms of the *local volume-fraction variance* $\sigma_V^2(R)$ associated with a spherical window of radius R. Specifically, a hyperuniform two-phase system is one in which $\sigma_V^2(R)$ decays faster than R^{-d} in the large-R regime,[24,43] i.e.

$$\lim_{R\to\infty} R^d \sigma_V^2(R) = 0 \tag{2}$$

In addition to having a direct-space representation,[45] the local variance $\sigma_V^2(R)$ has the following Fourier representation in terms of the spectral density $\tilde{\chi}_V(\mathbf{k})$:[24,43]

$$\sigma_V^2(R) = \frac{1}{v_1(R)(2\pi)^d} \int_{\mathbb{R}^d} \tilde{\chi}_V(\mathbf{k}) \tilde{\alpha}_2(k;R) d\mathbf{k} \tag{3}$$

where $v_1(R) = \pi^{d/2} R^d / \Gamma(d/2 + 1)$ is the volume of a d-dimensional sphere of radius R, $\Gamma(x)$ is the gamma function

$$\tilde{\alpha}_2(k;R) \equiv 2^d \pi^{d/2} \Gamma\left(\frac{d}{2}+1\right) \frac{J_{d/2}(kR)^2}{k^d} \tag{4}$$

is the Fourier transform of the scaled intersection volume of two spheres of radius R whose centers are separated by a distance r,[23] and $k \equiv |\mathbf{k}|$ is the wavenumber. The bottom panel of Figure 3 depicts the local variances corresponding to the spectral densities shown in the top panel.

As in the case of hyperuniform point configurations,[23,43] there are three different scaling regimes (classes) that describe the associated large-R behaviors of the volume-fraction variance when the spectral density goes to zero with the following power-law scaling:[24,43,46]

$$\tilde{\chi}_V(\mathbf{k}) \sim |\mathbf{k}|^\alpha \quad (k \to 0) \tag{5}$$

namely,

$$\sigma_V^2(R) \sim \begin{cases} R^{-(d+1)}, & \alpha > 1 \quad \text{(Class I)} \\ R^{-(d+1)} \ln R, & \alpha = 1 \quad \text{(Class II)} \\ R^{-(d+\alpha)}, & 0 < \alpha < 1 \quad \text{(Class III)} \end{cases} \tag{6}$$

where the exponent α is a positive constant. Classes I and III are the strongest and weakest forms of hyperuniformity, respectively. Stealthy hyperuniform media are also of class I

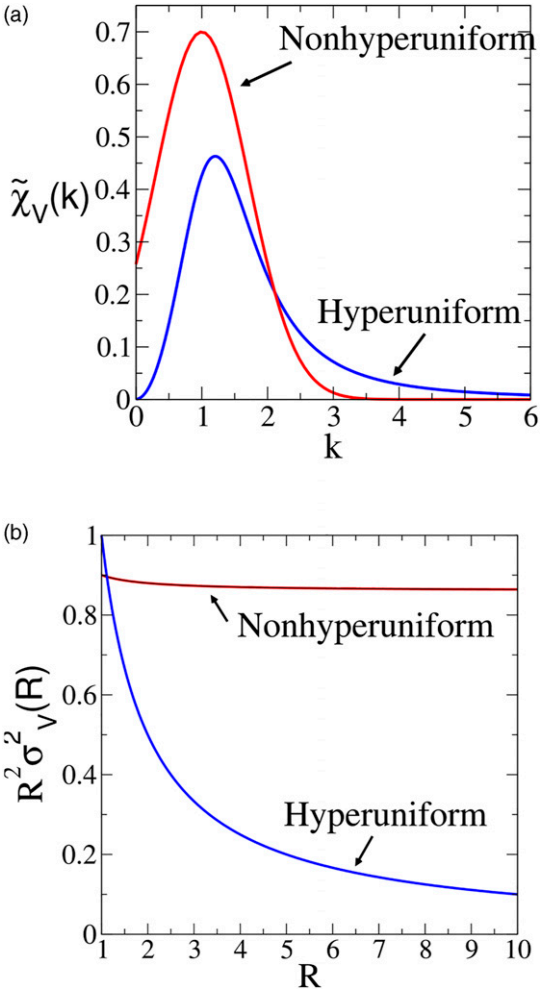

Figure 3. (a) Spectral densities versus wavenumber k for 2D nonhyperuniform and hyperuniform media (b) Corresponding local variances (multiplied by R^2) versus window radius R.

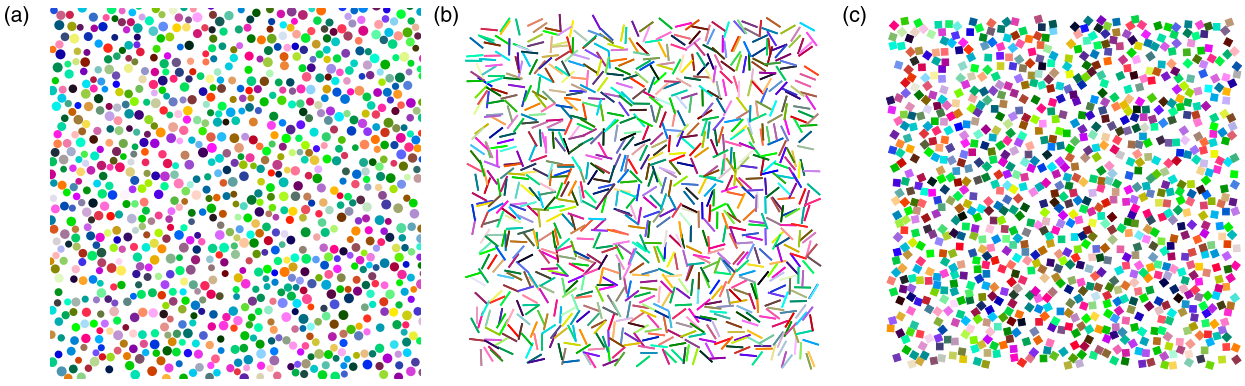

Figure 4. Representative images of 2D hyperuniform absorbing-state particle configurations, as adapted from Ref. 53. (a) Disks with continuous size distribution. (b) Identical needles. (c) Identical squares.

and are defined to be those that possess zero-scattering intensity for a set of wavevectors around the origin,[46] i.e.

$$\tilde{\chi}_V(\mathbf{k}) = 0 \quad \text{for } 0 \le |\mathbf{k}| \le K \tag{7}$$

Examples of such media are periodic packings of spheres as well as unusual disordered sphere packings derived from stealthy point patterns.[30,46]

By contrast, for any nonhyperuniform two-phase system, it is straightforward to show, using a similar analysis as for point configurations,[47] that the local variance has the following large-R scaling behaviors

$$\sigma_V^2(R) \sim \begin{cases} R^{-d}, & \alpha = 0 \quad \text{(typical nonhyperuniform)} \\ R^{-(d+\alpha)}, & -d < \alpha < 0 \quad \text{(antihyperuniform)} \end{cases} \tag{8}$$

For a "typical" nonhyperuniform system, $\tilde{\chi}_V(0)$ is bounded.[24] In *antihyperuniform* systems, $\tilde{\chi}_V(0)$ is unbounded, i.e.

$$\lim_{|\mathbf{k}| \to 0} \tilde{\chi}_V(\mathbf{k}) = +\infty \tag{9}$$

and hence are diametrically opposite to hyperuniform systems. Antihyperuniform systems include systems at thermal critical points (e.g. liquid-vapor and magnetic critical points),[48,49] fractals,[50] disordered non-fractals,[51] and certain substitution tilings.[52]

Forward approaches to generating disordered hyperuniform two-phase media

Here we describe "forward" (direct) approaches that have yielded disordered hyperuniform particulate media. Jammed as well as unjammed states are briefly reviewed.

Torquato and Stillinger[23] suggested that certain defect-free strictly jammed (i.e. mechanically stable) packings of identical spheres are hyperuniform. Specifically, they conjectured that any strictly jammed saturated infinite packing of identical spheres is hyperuniform. A saturated packing of hard spheres is one in which there is no space available to add another sphere. This conjecture was confirmed by Donev et al.[54] via a numerically generated maximally random jammed (MRJ) packing[55,56] of 10^6 hard spheres in three dimensions. Subsequently, the hyperuniformity of other MRJ hard-particle packings, including nonspherical particle shapes, was established across dimensions.[57–68] Jammed athermal soft-sphere models of granular media,[69,70] jammed thermal colloidal packings,[71,72] and jammed bidisperse emulsions[73] were also shown to be effectively hyperuniform. The singular transport and electromagnetic properties of MRJ packings of spheres[74] and superballs[68] have also been investigated.

Periodically driven colloidal suspensions were observed to have a phase transition in terms of the reversibility of the dynamics one decade ago.[75] Random organization models capture the salient physics of how driven systems can self-organize.[76] A subsequent study of random organization models of monodisperse (i.e. identical) spherical particles have shown that a hyperuniform state is achievable when a granular system goes through an absorbing phase transition to a critical state.[77] Many variants of such models and systems have been studied numerically.[78–82] To what extent is hyperuniformity is preserved when the model is generalized to particles with a size distribution and/or nonspherical shapes? This question was probed in a recent study[53] by examining disks with a size distribution, needle-like shapes and squares in two dimensions and it was demonstrated that their critical states are hyperuniform as two-phase media (see Figure 4). These results suggest that general particle systems subject to random organization can be a robust way to fabricate a wide class of hyperuniform states of matter by tuning the structures via different particle-size and -shape distributions. This tunability

capacity in turn potentially enables the creation of multifunctional hyperuniform materials with desirable optical, transport, and mechanical properties.

While there has been growing interest in disordered hyperuniform materials states, an obstacle has been an inability to produce large samples that are perfectly hyperuniform due to practical limitations of conventional numerical and experimental methods. To overcome these limitations, a general theoretical methodology has been developed to construct perfectly hyperuniform packings in d-dimensional Euclidean space $\mathbb{R}^d$.[83,84] Specifically, beginning with an initial general tessellation of space by disjoint cells that meets a "bounded-cell" condition, hard particles are placed inside each cell such that the local-cell particle packing fractions are identical to the global packing fraction; see Figure 5. It was proved that the constructed packings with a polydispersity in size in $\mathbb{R}^d$ are perfectly hyperuniform of class I in the infinite-sample-size limit, even though the initial point configuration that underlies the Voronoi tessellation is nonhyperuniform. Implementing this methodology in sphere tessellations of space (requiring spheres down to the infinitessimally small), establishes the hyperuniformity of the classical Hashin-Shtrikman multiscale coated-spheres structures, which are known to be two-phase media microstructures that possess optimal effective transport and elastic properties.[85,86] Figure 6 shows portions of 2D and 3D hyperuniform polydisperse packings that were converted from the corresponding Voronoi tessellations of nonhyperuniform random sequential addition (RSA) packings.[87] These computationally-designed microstructures can be fabricated via either photolithographic and 3D-printing techniques.[88–91]

Inverse approaches to generating disordered hyperuniform two-phase media

Here, we describe inverse optimization techniques that enable one to design microstructures with targeted spectral densities. These procedures include the capacity to tune the value of the power-law exponent $\alpha > 0$, defined by relation (5), for nonstealthy hyperuniform media as well as to design stealthy hyperuniform media, defined by relation (7).

The Yeong-Torquato stochastic optimization procedure[92,93] is a popular algorithm that has been employed to construct or reconstruct digitized multi-phase media from a prescribed set of different correlation functions in physical (direct) space.[34,94–100] A fictitious "energy" is defined to be a sum of squared differences between the target and simulated correlation function. The Yeong-Torquato procedure treats the construction or reconstruction task as an energy-minimization problem that it solves via simulated annealing. The Yeong-Torquato procedure was generalized to construct disordered hyperuniform materials with desirable effective macroscopic properties but from targeted structural information in Fourier (reciprocal) space, namely, the spectral density $\tilde{\chi}_V(\mathbf{k})$.[35] Specifically, the fictitious "energy" E of the system in d-dimensional Euclidean space $\mathbb{R}^d$ is defined as the following sum over wavevectors

$$E = \sum_{\mathbf{k}} \left[\frac{\tilde{\chi}_V(\mathbf{k})}{l^d} - \frac{\tilde{\chi}_{V,0}(\mathbf{k})}{l^d} \right]^2 \tag{10}$$

where the sum is over discrete wave vectors $\mathbf{k}$, $\tilde{\chi}_{V,0}(\mathbf{k})$ and $\tilde{\chi}_V(\mathbf{k})$ are the spectral densities of the target and (re) constructed microstructures, respectively, d is the space dimension, and l is the relevant characteristic length of the system used to scale the spectral densities such that they are dimensionless. As in the standard Yeong-Torquato procedure,[92,93] the simulated-annealing method is used to minimize the energy (10). It was demonstrated that one can design nonstealthy hyperuniform media and stealthy hyperuniform media with this Fourier-based inverse technique.[35] Such *in-silico* designed microstructures can be readily realized by 3D printing and lithographic technologies.[89]

Figure 7 shows designed realizations of digitized nonstealthy hyperuniform media with prescribed values of the power-law exponent $\alpha > 0$, defined by relation (5), at different values of the phase volume fraction ϕ.[35] It is seen that these designed materials possess a variety of morphologies: as ϕ increases for fixed α, the microstructures transition from particulate media consisting of isolated "particles" to labyrinth-like microstructures. Moreover, as α increases for fixed ϕ, short-range order increases in these hyperuniform materials.

The "collective-coordinate" optimization procedure represents a powerful reciprocal-space-based approach to generate disordered stealthy hyperuniform point configurations[101–103] as well as nonstealthy hyperuniform point configurations[104,105] in d-dimensional Euclidean space $\mathbb{R}^d$. In the case of the former, their degree of the stealthiness can be tuned by varying a dimensionless parameter χ, which measures the relative number of independently constrained degrees of freedom for wavenumbers up to the cut-off value K. For the range $0 < \chi < 1/2$, the stealthy states are disordered, and degree of short-range order increases as χ approaches 1/2.[106] Such stealthy point patterns can be decorated by nonoverlapping spheres, enabling the generation of *nondigitized* stealthy sphere packings, which have been used to model disordered two-phase composites that are both stealthy and hyperuniform,[16,30] as defined by relation (7). As we will see in Novel multifunctional disordered hyperuniform composites and porous media, stealthy hyperuniform composites are endowed with novel multifunctional characteristics.

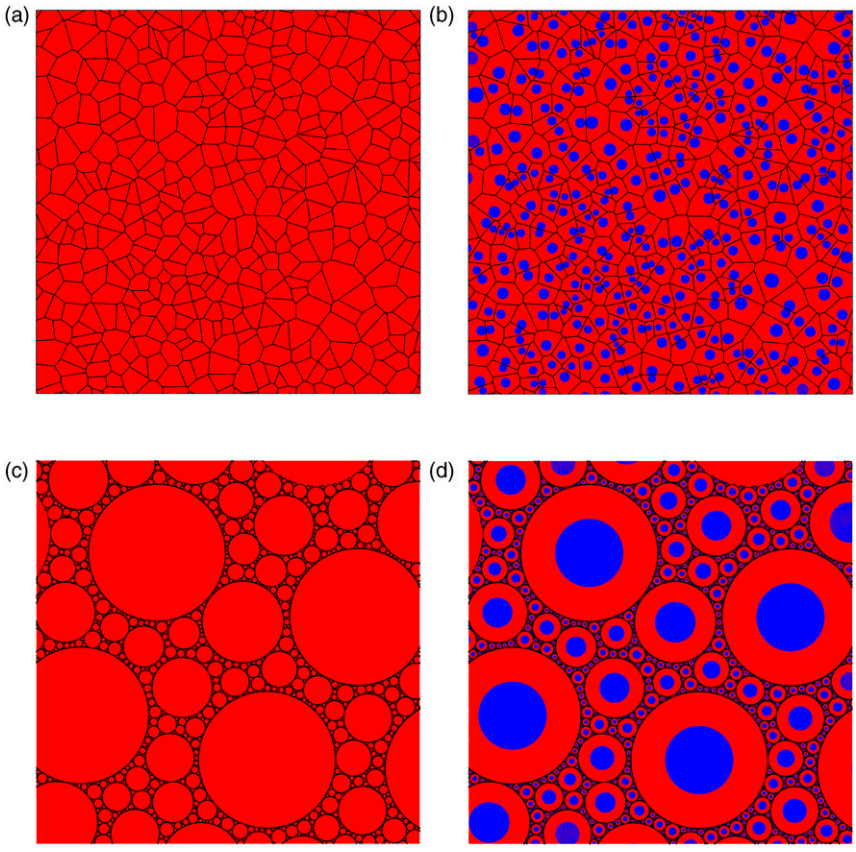

Figure 5. (a) A Voronoi tesselation of a nonhyperuniform disordered point configuration. (b) The disordered hyperuniform packing of spheres with a size distribution that results by adding particles in the Voronoi tesselation while ensuring that the local cell packing fraction is equal to global packing fraction. (c) A tessellation of space by spheres. (d) The Hashin-Shtrikman composite sphere assemblage that results by adding particles in the sphere tessellation while ensuring that the local cell packing fraction is equal to global packing fraction. These images are adapted from those in Ref. 83.

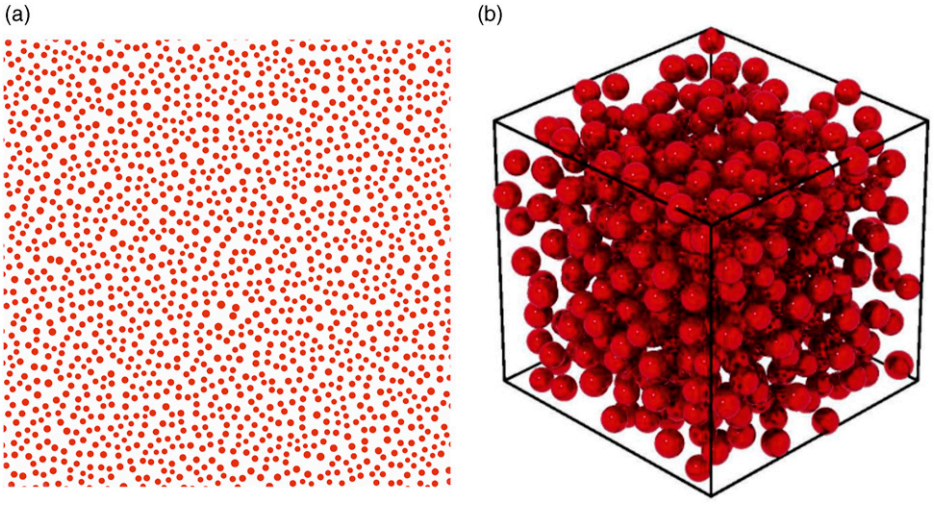

Figure 6. (a) A portion of a hyperuniform disk packing that was converted from a 2D RSA packing with the packing fraction ϕ_{init} = 0.41,025. (b) A portion of a hyperuniform sphere packing that was converted from a 3D saturated RSA packing with the packing fraction ϕ_{init} = 0.288. This figure is adapted from Ref. 83.

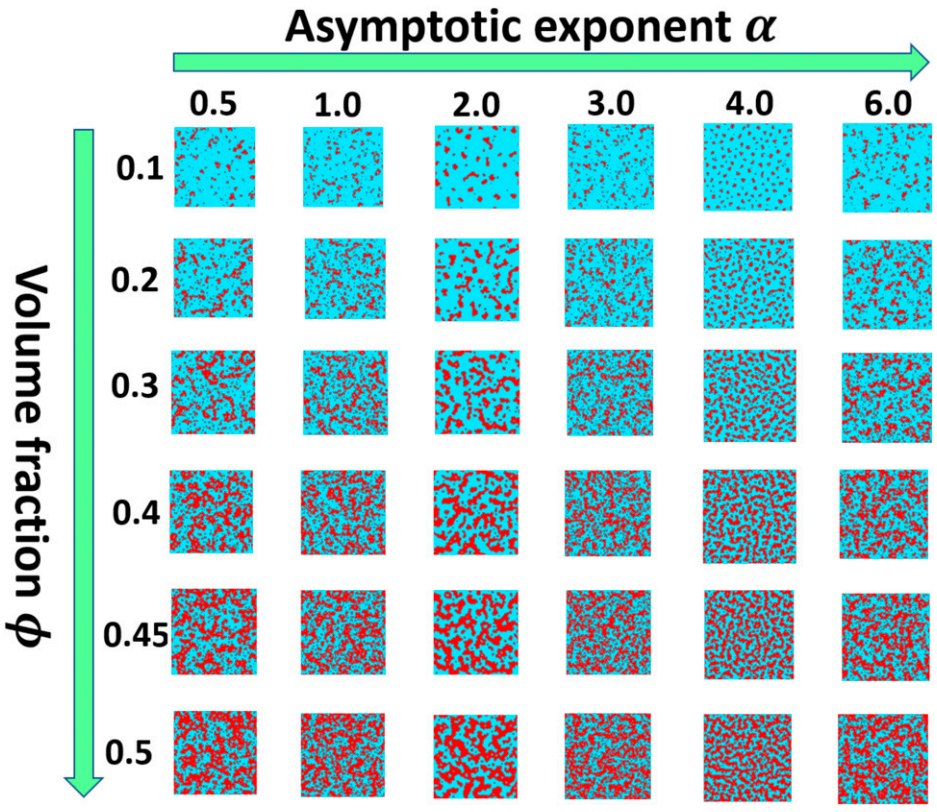

Figure 7. Realizations of disordered hyperuniform two-phase materials for different values of the volume fraction ϕ and the positive exponent α, defined by the spectral-density scaling law (5). This figure is adapted from Ref. 35.

Order metrics for disordered hyperuniform two-phase media

An outstanding open problem is the determination of appropriate "order metrics" to characterize the degree of large-scale order of both hyperuniform and nonhyperuniform media. This task is a highly challenging due to the infinite variety of possible two-phase microstructures (geometries and topologies). To begin such a program, the local variance $\sigma_V^2(R)$ was recently studied for a certain subset of class I hyperuniform media, including 2D periodic cellular networks as well as 2D periodic and disordered/irregular packings, some of which maximize their effective transport and elastic properties.[107] In particular, Kim and Torquato[107] evaluated the local variance $\sigma_V^2(R)$ as a function of the window radius R. They also computed the hyperuniformity order metric $\overline{B}_V$, i.e., the implied coefficient multiplying $R^{-(d+1)}$ in (6), for all of these class I 2D models to rank them according to their degree of order at a fixed volume fraction. The smaller is the value of $\overline{B}_V$, the more ordered is the microstructure with respect to large-scale volume-fraction fluctuations. Among the cellular networks considered, the honeycomb networks have the minimal values of the hyperuniformity order metrics $\overline{B}_V$ across all volume fractions. Among all structures studied there, triangular-lattice packings of circular disks have the minimal values of the order metric for almost all volume fractions.

It is desired to formulate order metrics to characterize the degree of order/disorder of the microstructures of two-phase media in d-dimensional Euclidean space $\mathbb{R}^d$ across length scales. It has recently been proposed that the local volume-fraction variance $\sigma_V^2(R)$ be used as an order metric for disordered and ordered two-phase media across all length scales by tracking it as a function of R.[108] The local variance $\sigma_V^2(R)$ as a function of R was determined for 22 different models across the first three space dimensions, including both hyperuniform and nonhyperuniform systems with varying degrees of short- and long-range order. It was found that the local volume-fraction variance as well as the asymptotic coefficients and integral measures derived from it provide reasonably robust and sensitive order metrics to categorize disordered and ordered two-phase media across all length scales. Such order metrics could be employed to accelerate the discovery of novel heterogeneous materials by tailoring their degree of order/disorder.

Novel multifunctional disordered hyperuniform composites and porous media

By mapping relatively large 2D disordered stealthy hyperuniform point configurations, obtained via the collective-coordinate optimization procedure,[101,102] to certain 2D trivalent dielectric networks via a Delaunay centroidal tessellation,[25] what was thought to be impossible at the time became possible. Specifically, the first disordered network solids to have large *complete* (both polarizations and blocking all directions) photonic band gaps comparable in size to those in photonic crystals were identified, but with the additional advantage of perfect isotropy.[25] The computational designs consist of trivalent networks of cell walls with circular cylinders at the nodes. The band structure was computed as a function of the degree of stealthiness χ (left panel of Figure 8) and the case of χ nearly equal to 0.5 (with an accompanying substantial degree of short-range order) leads to the maximal complete band-gap size in disordered hyperuniform dielectric networks. This numerical investigation enabled the design and fabrication of disordered cellular solids with the predicted photonic band-gap characteristics for the microwave regime (right panel of Figure 8), enabling unprecedented free-form waveguide geometries unhindered by crystallinity and anisotropy, and robust to defects.[109,110] Subsequently, stealthy hyperuniform materials were shown to have novel electromagnetic and elastic wave propagation characteristics, including transparency to long-wavelength radiation,[16,28,33,111,112] tunable diffusive and localization regimes,[33] enhanced absorption of waves,[113] and singular phononic band gaps.[32,39,114]

The effective thermal or electrical conductivities and elastic moduli of various 2D ordered and disordered hyperuniform cellular networks were studied.[115] The multifunctionality of a class of such low-density networks was established by demonstrating that they maximize or virtually maximize the effective conductivities and elastic

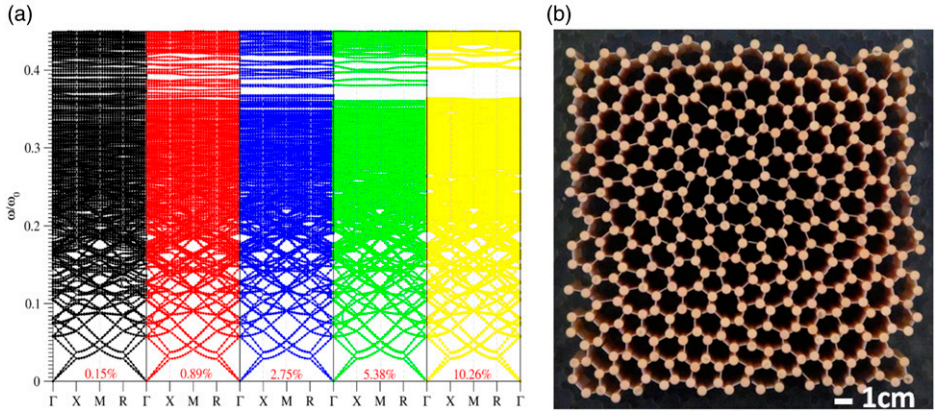

Figure 8. (a) Band structure for stealthy hyperuniform networks as a function of χ, as predicted from the computational study in Ref. 25. From left to right, χ = 0.1, 0.2, 0.3, 0.4 and 0.5. The relative band-gap size, measured by $\Delta\omega/\omega_C$ takes on the largest value of 10.26% for the rightmost case of χ = 0.5. (b) 3D fabrication of the computationally-designed maximal band-gap structure looking down from the top, as adapted from Ref. 110. The solid phase is aluminum oxide.

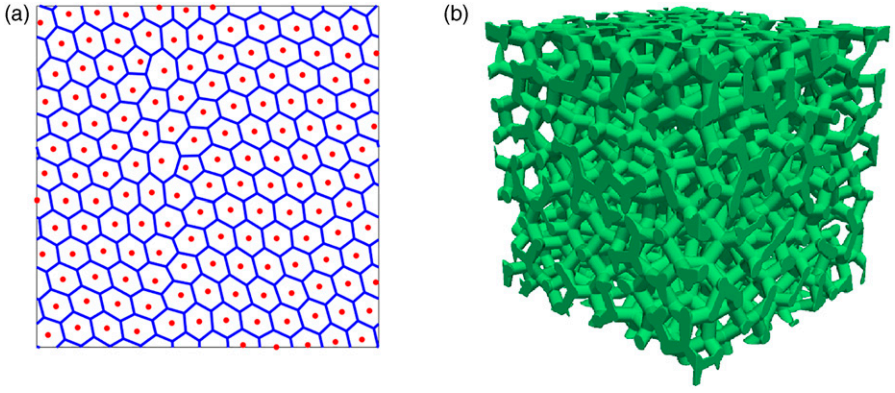

Figure 9. (a) 2D disordered hyperuniform trivalent network, as adapted from Ref. 115. (b) 3D disordered hyperuniform tetrahedrally-coordinated network, as adapted from Ref. 116.

moduli. This was accomplished by using the machinery of homogenization theory, including optimal bounds and cross-property bounds, and statistical mechanics. It was rigorously proved that anisotropic networks consisting of sets of intersecting parallel channels in the low-density limit, ordered or disordered, possess optimal effective conductivity tensors. For a variety of different disordered networks, it was shown that when short-range and long-range order increases, there is an increase in both the effective conductivity and elastic moduli of the network. Moreover, it was demonstrated that the effective conductivity and elastic moduli of various disordered networks (derived from disordered "stealthy" hyperuniform point patterns), such as the one shown in the left panel of Figure 9), possess virtually optimal values. Interestingly, the optimal networks for conductivity are also optimal for the fluid permeability associated with slow viscous flow through the channels as well as the mean survival time associated with diffusion-controlled reactions in the channels. 3D disordered hyperuniform networks, such as the one shown in right panel of Figure 9, have been shown to have sizable photonic band gaps.[116] In summary, 2D and 3D disordered hyperuniform low-weight cellular networks are multifunctional with respect to transport (e.g. heat dissipation and fluid transport), mechanical and electromagnetic properties, which can be readily fabricated using 2D lithographic and 3D printing technologies.[88–91]

The theoretical problem of estimating the effective properties of multiphase composite media is an outstanding one and dates back to work by some of the luminaries of science, including Maxwell,[117] Lord Rayleigh,[118] and Einstein.[119] The preponderance of previous theoretical studies have focused on the determination of static effective properties (e.g. dielectric constant, elastic moduli and fluid permeability) using a variety of methods, including approximation schemes,[117,120–122] bounding techniques,[3,4,85,123–125] and exact series-expansion procedures.[126–129] Much less is known about the theoretical prediction of the effective dynamic dielectric constant tensor $\varepsilon_e(\mathbf{k}_I)$, where $\mathbf{k}_I$ is wavevector of the incident radiation. The strong-contrast formalism has recently been used to derive exact *nonlocal* expansions for $\varepsilon_e(\mathbf{k}_I)$ that exactly account for complete microstructural information and hence multiple scattering to all orders for the range of wavenumbers for which our extended homogenization theory applies, i.e., $0 \leq |\mathbf{k}_I|\ell \lesssim 1$ (where ℓ is a characteristic heterogeneity length scale).[112] Due to the fast-convergence properties of such expansions, their lower-order truncations yield accurate closed-form approximate formulas for $\varepsilon_e(\mathbf{k}_I)$ that depend on the spectral density $\tilde{\chi}_V(\mathbf{k})$. It was shown that disordered stealthy hyperuniform particulate composites exhibit novel wave characteristics, including the capacity to act as low-pass filters that transmit waves "isotropically" up to a selected wavenumber or refractive indices that abruptly change over a narrow range of wavenumbers. The aforementioned nonlocal formulas can now be used to accelerate the discovery of novel electromagnetic composites by appropriate tailoring of the spectral densities.

Cross-property relations for two-phase composite media were recently obtained that link effective elastic and electromagnetic wave characteristics to one another, including effective wave speeds and attenuation coefficients.[16] This was achieved by deriving accurate formulas for the effective elastodynamic properties[111] as well as effective electromagnetic properties,[112] each of which depend on the microstructure via the spectral density. Such formulas enable one to explore the wave characteristics of a broad class of disordered microstructures, including exotic disordered hyperuniform varieties. It was specifically demonstrated that disordered stealthy hyperuniform/nonhyperuniform microstructures exhibit novel elastic wave characteristics that have the potential for future applications, e.g. narrow-band or narrow-band-pass filters that absorb or transmit elastic waves isotropically for a narrow spectrum of frequencies, respectively. These cross-property relations for effective electromagnetic and elastic wave characteristics can be applied to design multifunctional composites (Figure 10), such as exterior components of spacecrafts or building materials that require both excellent stiffness and electromagnetic absorption, and heat-sinks for CPUs that have to efficiently emit thermal radiation and suppress mechanical vibrations, and nondestructive evaluation of the mechanical strength of materials from the effective dielectric response.

The effective transport characteristics of fluid-saturated porous media have been studied using certain rigorous microstructure-property relations.[130] Of particular interest were the predictions of the formation factor $\mathcal{F}$, mean survival time τ, principal nuclear magnetic resonance (NMR) (diffusion) relaxation time T_1, principal viscous relaxation time Θ_1, and fluid permeability k for hyperuniform and nonhyperuniform models of porous media. Among other results, a Fourier representation of a classic rigorous upper bound on the fluid permeability was derived that depends on the spectral density $\tilde{\chi}_V(\mathbf{k})$ to infer how the permeabilities of hyperuniform porous media perform relative to those of nonhyperuniform ones; see Figure 11. It was found that the velocity fields in nonhyperuniform porous media are generally much more localized over the pore space compared to those in their hyperuniform counterparts, which has certain implications for their permeabilities. Rigorous bounds on the transport properties $\mathcal{F}$, τ, T_1 and Θ_1 suggest a new approximate formula for the fluid permeability that provides reasonably accurate permeability predictions of a certain class of hyperuniform and nonhyperuniform porous media. These comparative studies shed new light on the microstructural characteristics, such as *pore-size statistics*, in determining the

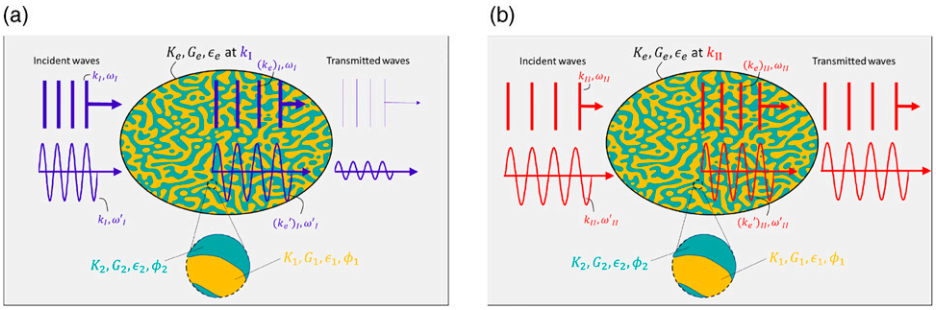

Figure 10. Schematics illustrating elastic and electromagnetic waves at two different wavenumbers (a) k_I and (b) k_{II} incident to, inside of and transmitted from a two-phase heterogeneous material (a large ellipse) consisting of a matrix phase (shown in yellow) and a dispersed phase (shown in cyan). Parallel lines and sinusoidal curves represent elastic and electromagnetic waves, respectively. (a) For an elastic wave with a wavenumber k_I, while the wavefronts inside this material experience microscopic disturbances, they effectively behave like a plane wave inside a homogeneous material with an effective wavenumber $(k_e)_I$ and effective elastic moduli K_e and G_e. Analogously, for an electromagnetic wave, this material behaves like a homogeneous material with an effective dielectric constant ϵ_e. For instance, both elastic and electromagnetic waves are attenuated due to scattering if this composite has a non-zero scattering intensity at k_I. (b) For waves (red) of a wavenumber k_{II}, this composite can be effectively transparent, if it has a zero-scattering intensity at k_{II}. This figure is adapted from Ref. 16.

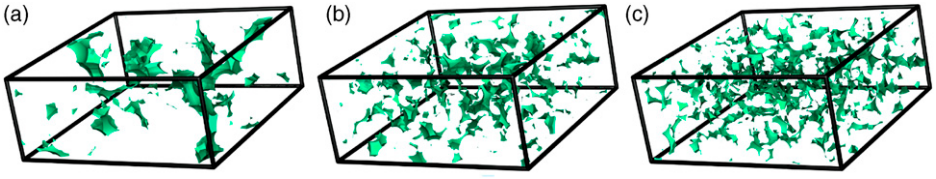

Figure 11. Images of the void space after applying a "dilation" operation to three different sphere packings, as adapted from Ref. 130. (a) A nonhyperuniform equilibrium packing. (b) A hyperuniform maximally random jammed packing. (c) A disordered stealthy packing.

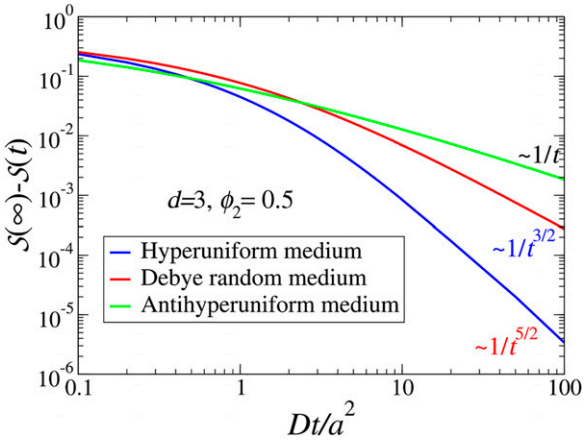

Figure 12. Excess spreadabilities versus dimensionless time Dt/a^2 for antihyperuniform media (top curve), Debye random media (middle curve), and disordered hyperuniform media (bottom curve) for $d = 3$ and $\phi_2 = 0.5$, as adapted from Ref. 132. The long-time inverse power-law scalings of $\mathcal{S}(\infty) - \mathcal{S}(t)$ for each of these models is indicated. Here a is a characteristic length scale for each model, as defined in Ref. 132.

transport properties of general porous media. In a more recent study, the second moment of the pore-size probability density function was shown to be correlated with the *critical pore radius*, which contains crucial *connectivity* information about the pore space.[131] All of these findings have important implications for the design of porous materials with desirable transport properties.

A new dynamic probe of the microstructure of two-phase media has been introduced called the *spreadability* $\mathcal{S}(t)$, which is a measure of the spreadability of diffusion information as a function of time t in any Euclidean space dimension d.[132] It is assumed that a solute at $t = 0$ is uniformly distributed throughout phase 2 with volume fraction ϕ_2, and completely absent from phase 1 with volume fraction ϕ_1, and each phase has same diffusion coefficient D. The spreadability is the fraction of the total amount of solute present that has diffused into phase 1 at time t. In particular, a three-dimensional formula due to Prager[133] was generalized to any dimension in direct space and its Fourier representation was derived. The latter is an

exact integral relation for the spreadability $\mathcal{S}(t)$ that depends only on the spectral density $\tilde{\chi}_V(\mathbf{k})$:

$$\mathcal{S}(\infty) - \mathcal{S}(t) = \frac{1}{(2\pi)^d \phi_2} \int_{\mathbb{R}^d} \tilde{\chi}_V(\mathbf{k}) \exp\left[-k^2 D t\right] d\mathbf{k} \geq 0 \quad (11)$$

where $\mathcal{S}(\infty) = \phi_1$. Importantly, the short-, intermediate- and long-time behaviors of $\mathcal{S}(t)$ contain crucial small-, intermediate- and large-scale structural characteristics. For hyperuniform media, it was shown that the "excess" spreadability, $\mathcal{S}(\infty) - \mathcal{S}(t)$, decays to its long-time behavior exponentially faster than that of any nonhyperuniform medium, the "slowest" being antihyperuniform media, as illustrated in Figure 12. It was also shown that there is a remarkable link between the spreadability and NMR pulsed field gradient spin-echo amplitude and diffusion MRI.[132] Elsewhere, this new theoretical/experimental tool was applied to characterize many different models and a porous-medium sample.[68,134]

Conclusions and outlook

We have seen that the exotic hybrid crystal-liquid structural attributes of disordered hyperuniform composites can be endowed with an array of extraordinary physical properties, including photonic, phononic, transport and mechanical characteristics that are only beginning to be discovered. Disordered hyperuniform media can have advantages over their periodic counterparts, such as unique or nearly optimal, direction-independent physical properties and robustness against defects. The field of hyperuniformity is still in its infancy, though, and a deeper fundamental understanding of these unusual states of matter is required in order to realize their full potential for next-generation materials. Future challenges include the further development of forward and inverse computational approaches to generate disordered hyperuniform structures, formulation of improved order metrics to rank order them, and identifying their desirable multifunctional characteristics. These computational designs can subsequently be combined with the 2D lithographic fabrication techniques[91] and 3D additive manufacturing techniques[88–90] to accelerate the discovery of novel multifunctional hyperuniform two-phase materials.

Cross-property "maps" have recently been introduced to connect combinations of pairs of effective static transport and elastic properties of general particulate media via analytical structure-property formulas.[135] Cross-property maps and their extensions will facilitate the rational design of composites with different desirable multifunctional characteristics. In future work, it would be valuable to formulate cross-property maps for the various physical properties described in Novel multifunctional disordered hyperuniform composites and porous media using the corresponding analytical estimates of these properties in order to aid in the multifunctional design of disordered hyperuniform composites.

To complement rigorous approaches to estimate the macroscopic properties of heterogeneous media from the microstructure, data-driven methodologies to establish structure-property relationships are increasingly being employed.[99,136–138] The rapid increase in computational resources facilitates the calculation of effective properties for very large data sets (thousands or more) of different microstructures, including those obtained experimentally via 2D and 3D high-resolution imaging techniques.[3,139–142] As a result, it has become manageable to generate large numbers of realistic virtual microstructures, and using those to perform exploratory computational screening of structure–property relationships. The application of machine-learning and other data-driven approaches for the discovery of multifunctional disordered hyperuniform composites has yet to be undertaken and hence is a promising avenue for future research.

Acknowledgements

The author thanks Jaeuk Kim, Charles Maher, Murray Skolnick and Haina Wang for valuable comments about the paper. The author gratefully acknowledges the support of the Air Force Office of Scientific Research Program on Mechanics of Multifunctional Materials and Microsystems under award No. FA9550-18-1-0514.

Declaration of conflicting interests

The author(s) declared no potential conflicts of interest with respect to the research, authorship, and/or publication of this article.

Funding

The author(s) disclosed receipt of the following financial support for the research, authorship, and/or publication of this article: This work was supported by Air Force Office of Scientific Research (FA9550-18-1-0514).

ORCID iD

Salvatore Torquato https://orcid.org/0000-0003-4614-335X

References

1. Christensen RM. *Mechanics of composite materials*. New York: Wiley, 1979.
2. Nemat-Nasser S and Micromechanics HM. *Overall properties of heterogeneous materials*. Amsterdam: North-Holland, 1993.
3. Torquato S. *Random heterogeneous materials: microstructure and macroscopic properties*. New York: Springer-Verlag, 2002.

4. Milton GW. *The theory of composites*. Cambridge, England: Cambridge University Press, 2002.
5. Sahimi M. *Heterogeneous materials I: linear transport and optical properties*. New York: Springer-Verlag, 2003.
6. Bergman DJ. The dielectric constant of a composite material– A problem in classical physics. *Phys Rep C* 1978; 43: 377–407.
7. Avellaneda M, Cherkaev AV, Lurie KA, et al. On the effective conductivity of polycrystals and a three-dimensional phase-interchange inequality. *J Appl Phys* 1988; 63: 4989–5003.
8. Torquato S. Relationship between permeability and diffusion-controlled trapping constant of porous media. *Phys Rev Lett* 1990; 64: 2644–2646.
9. Torquato S and Avellaneda M. Diffusion and reaction in heterogeneous media: pore size distribution, relaxation times, and mean survival time. *J Chem Phys* 1991; 95: 6477–6489.
10. Avellaneda M and Torquato S. Rigorous link between fluid permeability, electrical conductivity, and relaxation times for transport in porous media. *Phys Fluids A* 1991; 3: 2529–2540.
11. Gibiansky LV and Torquato S. Rigorous link between the conductivity and elastic moduli of fibre-reinforced composite materials. *Phil Trans R Soc Lond A* 1995; 353: 243–278.
12. Gibiansky LV and Torquato S. Connection between the conductivity and bulk modulus of isotropic composite materials. *Proc R Soc Lond A* 1996; 452: 253–283.
13. Gibiansky LV and Torquato S. Thermal expansion of isotropic multiphase composites and polycrystals. *J Mech Phys Sol* 1997; 45: 1223–1252.
14. Torquato S and Donev A. Minimal surfaces and multifunctionality. *Proc R Soc Lond A* 2004; 460: 1849–1856.
15. Sevostianov I and Kachanov M. Connections between elastic and conductive properties of heterogeneous materials. In: *Advances in Applied Mechanics*. Vol. 42. Cham: Elsevier, 2009, pp. 69–252.
16. Kim J and Torquato S. Multifunctional composites for elastic and electromagnetic wave propagation. *Proc Nat Acad Sci* 2020; 117: 8764–8774.
17. Bendsøe MP and Kikuchi N. Generating optimal topologies in structural design using a homogenization method. *Comput Methods Appl Mech Eng* 1988; 71: 197–224.
18. Sigmund O and Torquato S. Design of materials with extreme thermal expansion using a three-phase topology optimization method. *J Mech Phys Sol* 1997; 45: 1037–1067.
19. Torquato S, Hyun S and Donev A. Multifunctional composites: optimizing microstructures for simultaneous transport of heat and electricity. *Phys Rev Lett* 2002; 89: 266601.
20. Sigmund O and Sondergaard JJ. Systematic design of phononic band-gap materials and structures by topology optimization. *Phil Trans R Soc Lond A* 2003; 100: 1001–1019.
21. Torquato S. Optimal design of heterogeneous materials. *Ann Rev Mater Res* 2010; 40: 101–129.
22. Yu S, Qiu CW, Chong Y, et al. Engineered disorder in photonics. *Nat Rev Mater* 2021; 6: 226–243.
23. Torquato S and Stillinger FH. Local density fluctuations, hyperuniform systems, and order metrics. *Phys Rev E* 2003; 68: 041113.
24. Torquato S. Hyperuniform states of matter. *Phys Rep* 2018; 745: 1–95.
25. Florescu M, Torquato S, Steinhardt PJ, et al. Designer disordered materials with large complete photonic band gaps. *Proc Nat Acad Sci* 2009; 106: 20658–20663.
26. Jiao Y, Lau T, Hatzikirou H, et al. Avian photoreceptor patterns represent a disordered hyperuniform solution to a multiscale packing problem. *Phys Rev E* 2014; 89: 022721.
27. De Rosa C, Auriemma F, Diletto C, et al. Toward hyperuniform disordered plasmonic nanostructures for reproducible surface-enhanced Raman spectroscopy. *Phys Chem Chem Phys* 2015; 17: 8061–8069.
28. Leseur O, Pierrat R, Carminati R, et al. High-density hyperuniform materials can be transparent. *Optica* 2016; 3: 763–767.
29. Ma T, Guerboukha H, Girard M, et al. 3D printed hollow-core terahertz optical waveguides with hyperuniform disordered dielectric reflectors. *Adv Opt Mater* 2016; 4: 2085–2094.
30. Zhang G, Stillinger FH, Torquato S, et al. Transport, geometrical and topological properties of stealthy disordered hyperuniform two-phase systems. *J Chem Phys* 2016; 145: 244109.
31. Zhou W, Cheng Z, Zhu B, et al. Hyperuniform disordered network polarizers. *IEEE J Select Top Quan Elec* 2016; 22: 288–294.
32. Gkantzounis G, Amoah T, Florescu M, et al. Hyperuniform disordered phononic structures. *Phys Rev B* 2017; 95: 094120.
33. Froufe-Pérez LS, Engel M, José Sáenz J, et al. Transport phase diagram and anderson localization in hyperuniform disordered photonic materials. *Proc Nat Acad Sci* 2017; 114: 9570–9574.
34. Xu Y, Chen S, Chen PE, et al. Microstructure and mechanical properties of hyperuniform heterogeneous materials. *Phys Rev E* 2017; 96: 043301.
35. Chen D and Torquato S. Designing disordered hyperuniform two-phase materials with novel physical properties. *Acta Mater* 2018; 142: 152–161.
36. Zhang H, Chu H, Giddens H, et al. Experimental demonstration of luneburg lens based on hyperuniform disordered media. *Appl Phys Lett* 2019; 114: 053507.
37. Gorsky S, Britton WA, Chen Y, et al. Engineered hyperuniformity for directional light extraction. *APL Photon* 2019; 4: 110801.

38. Sheremet A, Pierrat R, Carminati R, et al. Absorption of scalar waves in correlated disordered media and its maximization using stealth hyperuniformity. *Phys Rev A* 2020; 101: 053829.
39. Rohfritsch A, Conoir JM, Valier-Brasier T, et al. Impact of particle size and multiple scattering on the propagation of waves in stealthy-hyperuniform media. *Phys Rev E* 2020; 102: 053001.
40. Zhang H, Cheng Q, Chu H, et al. Hyperuniform disordered distribution metasurface for scattering reduction. *Appl Phys Lett* 2021; 118: 101601.
41. Granchi N, Spalding R, Lodde M, et al. Near-field investigation of luminescent hyperuniform disordered materials. *Adv Opt Mater* 2022; 10: 2102565.
42. Aeby S, Aubry GJ, Froufe-Pérez LS, et al. Fabrication of hyperuniform dielectric networks via heat-induced shrinkage reveals a bandgap at telecom wavelengths. *Adv Opt Mater* 2022; 2022: 2200232.
43. Zachary CE and Torquato S. Hyperuniformity in point patterns and two-phase heterogeneous media. *J Stat Mech Theor Exp* 2009; 2009: P12015.
44. Debye P, Anderson HR, Brumberger H, et al. Scattering by an inhomogeneous solid. II. The correlation function and its applications. *J Appl Phys* 1957; 28: 679–683.
45. Lu BL and Torquato S. Local volume fraction fluctuations in heterogeneous media. *J Chem Phys* 1990; 93: 3452–3459.
46. Torquato S. Disordered hyperuniform heterogeneous materials. *J Phys Cond Mat* 2016; 28: 414012.
47. Torquato S. Structural characterization of many-particle systems on approach to hyperuniform states. *Phys Rev E* 2021; 103: 052126.
48. Stanley HE. *Introduction to phase transitions and critical phenomena*. New York: Oxford University Press, 1987.
49. Binney JJ, Dowrick NJ, Fisher AJ, et al. *The theory of critical phenomena: an introduction to the renormalization group*. Oxford, England: Oxford University Press, 1992.
50. Mandelbrot BB. *The fractal geometry of nature*. New York: W. H. Freeman, 1982.
51. Torquato S, Kim J, Klatt MA, et al. Local number fluctuations in hyperuniform and nonhyperuniform systems: higher-order moments and distribution functions. *Phys Rev X* 2021; 11: 021028.
52. Oğuz EC, Socolar JES, Steinhardt PJ, et al. Hyperuniformity and anti-hyperuniformity in one-dimensional substitution tilings. *Acta Cryst Sec A Found Adv* 2019; A75: 3–13.
53. Ma Z and Torquato S. Hyperuniformity of generalized random organization models. *Phys Rev E* 2019; 99: 022115.
54. Donev A, Stillinger FH, Torquato S, et al. Unexpected density fluctuations in disordered jammed hard-sphere packings. *Phys Rev Lett* 2005; 95: 090604.
55. Torquato S, Truskett TM, Debenedetti PG, et al. Is random close packing of spheres well defined? *Phys Rev Lett* 2000; 84: 2064–2067.
56. Torquato S. Perspective: basic understanding of condensed phases of matter via packing models. *J Chem Phys* 2018; 149: 020901.
57. Skoge M, Donev A, Stillinger FH, et al. Packing hyperspheres in high-dimensional Euclidean spaces. *Phys Rev E* 2006; 74: 041127.
58. Jiao Y, Stillinger FH, Torquato S, et al. Distinctive features arising in maximally random jammed packings of superballs. *Phys Rev E* 2010; 81: 041304.
59. Zachary CE, Jiao Y, Torquato S, et al. Hyperuniform long-range correlations are a signature of disordered jammed hard-particle packings. *Phys Rev Lett* 2011; 106: 178001.
60. Jiao Y and Torquato S. Maximally random jammed packings of Platonic solids: hyperuniform long-range correlations and isostaticity. *Phys Rev E* 2011; 84: 041309.
61. Hopkins AB, Stillinger FH, Torquato S, et al. Nonequilibrium static diverging length scales on approaching a prototypical model glassy state. *Phys Rev E* 2012; 86: 021505.
62. Chen D, Jiao Y, Torquato S, et al. Equilibrium phase behavior and maximally random jammed state of truncated tetrahedra. *J Phys Chem B* 2014; 118: 7981–7992.
63. Tian J, Xu Y, Jiao Y, et al. A geometric-structure theory for maximally random jammed packings. *Sci Rep* 2015; 5: 16722.
64. Klatt MA and Torquato S. Characterization of maximally random jammed sphere packings. II. Correlation functions and density fluctuations. *Phys Rev E* 2016; 94: 022152.
65. Atkinson S, Zhang G, Hopkins AB, et al. Critical slowing down and hyperuniformity on approach to jamming. *Phys Rev E* 2016; 94: 012902.
66. Atkinson S, Stillinger FH, Torquato S, et al. Static structural signatures of nearly jammed disordered and ordered hard-sphere packings: direct correlation function. *Phys Rev E* 2016; 94: 032902.
67. Cinacchi G and Torquato S. Hard convex lens-shaped particles: metastable, glassy and jammed states. *Soft Matter* 2018; 14: 8205–8218.
68. Maher CE, Stillinger FH, Torquato S, et al. Characterization of void space, large-scale structure, and transport properties of maximally random jammed packings of superballs. *Phys Rev Mater* 2022; 6: 025603.
69. Silbert LE and Silbert M. Long-wavelength structural anomalies in jammed systems. *Phys Rev E* 2009; 80: 041304.
70. Berthier L, Chaudhuri P, Coulais C, et al. Suppressed compressibility at large scale in jammed packings of size-disperse spheres. *Phys Rev Lett* 2011; 106: 120601.
71. Kurita R and Weeks ER. Incompressibility of polydisperse random-close-packed colloidal particles. *Phys Rev E* 2011; 84: 030401.
72. Dreyfus R, Xu Y, Still T, et al. Diagnosing hyperuniformity in two-dimensional, disordered, jammed packings of soft spheres. *Phys Rev E* 2015; 91: 012302.

73. Ricouvier J, Pierrat R, Carminati R, et al. Optimizing hyperuniformity in self-assembled bidisperse emulsions. *Phys Rev Lett* 2017; 119: 208001.
74. Klatt MA and Torquato S. Characterization of maximally random jammed sphere packings. III. Transport and electromagnetic properties via correlation functions. *Phys Rev E* 2018; 97: 012118.
75. Pine DJ, Gollub JP, Brady JF, et al. Chaos and threshold for irreversibility in sheared suspensions. *Nature* 2005; 438: 997–1000.
76. Laurent C, Chaikin PM, Gollub JP, et al. Random organization in periodically driven systems. *Nat Phys* 2008; 4: 420–424.
77. Hexner D and Levine D. Hyperuniformity of critical absorbing states. *Phys Rev Lett* 2015; 114: 110602.
78. Hexner D and Levine D. Noise, diffusion, and hyperuniformity. *Phys Rev Lett* 2017; 118: 020601.
79. Tjhung E and Berthier L. Hyperuniform density fluctuations and diverging dynamic correlations in periodically driven colloidal suspensions. *Phys Rev Lett* 2015; 114: 148301.
80. Dickman R and da Cunha SD. Particle-density fluctuations and universality in the conserved stochastic sandpile. *Phys Rev E* 2015; 92: 020104.
81. Goldfriend T, Diamant H, Witten TA, et al. Screening, hyperuniformity, and instability in the sedimentation of irregular objects. *Phys Rev Lett* 2017; 118: 158005.
82. Wang J, Schwarz JM, Paulsen JD, et al. Hyperuniformity with no fine tuning in sheared sedimenting suspensions. *Nat Comm* 2018; 9: 1–7.
83. Kim J and Torquato S. Methodology to construct large realizations of perfectly hyperuniform disordered packings. *Phys Rev E* 2019; 99: 052141.
84. Kim J and Torquato S. New tessellation-based procedure to design perfectly hyperuniform disordered dispersions for materials discovery. *Acta Mater* 2019; 168: 143–151.
85. Hashin Z and Shtrikman S. A variational approach to the theory of the effective magnetic permeability of multiphase materials. *J Appl Phys* 1962; 33: 3125–3131.
86. Hashin Z and Shtrikman S. A variational approach to the elastic behavior of multiphase materials. *J Mech Phys Sol* 1963; 4: 286–295.
87. Torquato S, Uche OU, Stillinger FH, et al. Random sequential addition of hard spheres in high Euclidean dimensions. *Phys Rev E* 2006; 74: 061308.
88. Wong KV and Hernandez A. A review of additive manufacturing. *Int Scholar Res Notic* 2012; 2012: 1–10.
89. Vaezi M, Seitz H, Yang S, et al. A review on 3D micro-additive manufacturing technologies. *Int J Adv Manuf Technol* 2013; 67: 1721–1754.
90. Shirazi SFS, Gharehkhani S, Mehrali M, et al. A review on powder-based additive manufacturing for tissue engineering: selective laser sintering and inkjet 3d printing. *Sci Tech Adv Mater* 2015; 16: 033502.
91. Zhao K and Mason TG. Assembly of colloidal particles in solution. *Rep Prog Phys* 2018; 81: 126601.
92. Yeong CLY and Torquato S. Reconstructing random media. *Phys Rev E* 1998; 57: 495–506.
93. Yeong CLY and Torquato S. Reconstructing random media: II. Three-dimensional media from two-dimensional cuts. *Phys Rev E* 1998; 58: 224–233.
94. Jiao Y, Stillinger FH, Torquato S, et al. Modeling heterogeneous materials via two-point correlation functions: basic principles. *Phys Rev E* 2007; 76: 031110.
95. Jiao Y, Stillinger FH, Torquato S, et al. A superior descriptor of random textures and its predictive capacity. *Proc Nat Acad Sci* 2009; 106: 17634–17639.
96. Pant LM, Mitra SK, Secanell M, et al. Multigrid hierarchical simulated annealing method for reconstructing heterogeneous media. *Phys Rev E* 2015; 92: 063303.
97. Karsanina MV and Gerke KM. Hierarchical optimization: fast and robust multiscale stochastic reconstructions with rescaled correlation functions. *Phys Rev Lett* 2018; 121: 265501.
98. Čapek P. On the importance of simulated annealing algorithms for stochastic reconstruction constrained by low-order microstructural descriptors. *Trans Porous Media* 2018; 121: 59–80.
99. Li X, Zhang Y, Zhao H, et al. A transfer learning approach for microstructure reconstruction and structure-property predictions. *Sci Rep* 2018; 8: 13461.
100. Skolnick M and Torquato S. Understanding degeneracy of two-point correlation functions via debye random media. *Phys Rev E* 2021; 104: 045306.
101. Uche OU, Stillinger FH, Torquato S, et al. Constraints on collective density variables: two dimensions. *Phys Rev E* 2004; 70: 046122.
102. Batten RD, Stillinger FH, Torquato S, et al. Classical disordered ground states: super-ideal gases, and stealth and equi-luminous materials. *J Appl Phys* 2008; 104: 033504.
103. Zhang G, Stillinger F, Torquato S, et al. Ground states of stealthy hyperuniform potentials: I. Entropically favored configurations. *Phys Rev E* 2015; 92: 022119.
104. Uche OU, Torquato S, Stillinger FH, et al. Collective coordinates control of density distributions. *Phys Rev E* 2006; 74: 031104.
105. Zhang G, Stillinger FH, Torquato S, et al. The perfect glass paradigm: disordered hyperuniform glasses down to absolute zero. *Sci Rep* 2016; 6: 36963.
106. Torquato S, Zhang G, Stillinger FH, et al. Ensemble theory for stealthy hyperuniform disordered ground states. *Phys Rev X* 2015; 5: 021020.
107. Kim J and Torquato S. Characterizing the hyperuniformity of ordered and disordered two-phase media. *Phys Rev E* 2021; 103: 012123.
108. Torquato S, Skolnick M and Kim J. Local order metrics for two-phase media across length scales. *J Phys A: Math Theor* 2022; 55: 274003.

109. Florescu M, Steinhardt PJ, Torquato S, et al. Optical cavities and waveguides in hyperuniform disordered photonic solids. *Phys Rev B* 2013; 87: 165116.
110. Man W, Florescu M, Williamson EP, et al. Isotropic band gaps and freeform waveguides observed in hyperuniform disordered photonic solids. *Proc Nat Acad Sci* 2013; 110: 15886–15891.
111. Kim J and Torquato S. Effective elastic wave characteristics of composite media. *New J Phys* 2020; 22: 123050.
112. Torquato S and Kim J. Nonlocal effective electromagnetic wave characteristics of composite media: beyond the quasistatic regime. *Phys Rev X* 2021; 11: 021002.
113. Bigourdan F, Pierrat R, Carminati R, et al. Enhanced absorption of waves in stealth hyperuniform disordered media. *Opt Express* 2019; 27: 8666–8682.
114. Romero-García V, Lamothe N, Theocharis G, et al. Stealth acoustic materials. *Phys Rev Appl* 2019; 11: 054076.
115. Torquato S and Chen D. Multifunctional hyperuniform cellular networks: optimality, anisotropy and disorder. *Multifunc Mater* 2018; 1: 015001.
116. Klatt MA, Steinhardt PJ, Torquato S, et al. Gap sensitivity reveals universal behaviors in optimized photonic crystal and disordered networks. *Phys Rev Lett* 2021; 127: 037401.
117. Maxwell JC. *Treatise on electricity and magnetism*. Oxford: Clarendon Press, 1873.
118. Strutt JW. On the influence of obstacles arranged in a rectangular order upon the properties of medium. *Phil Mag* 1892; 34: 481–502.
119. Einstein A. Eine neue bestimmung der Moleküldimensionen. *Ann Phys* 1906; 19: 289–306.
120. Bruggeman D. Berechnung verschiedener Physikalischer Konstanten von heterogenen Substanzen. *Ann Physik* 1935; 24: 636–679.
121. Brinkman HC. A calculation of the viscous force exerted by a flowing fluid on a dense swarm of particles. *Appl Sci Res* 1947; A1: 27–34.
122. Budiansky B. On the elastic moduli of some heterogeneous materials. *J Mech Phys Sol* 1965; 13: 223–227.
123. Prager S. Viscous flow through porous media. *Phys Fluids* 1961; 4: 1477–1482.
124. Beran M. Use of the variational approach to determine bounds for the effective permittivity in random media. *Nuovo Cimento* 1965; 38: 771–782.
125. Kohn RV and Lipton R. Optimal bounds for the effective energy of a mixture of isotropic, incompressible elastic materials. *Arch R Mech Anal* 1988; 102: 331–350.
126. Brown WF. Solid mixture permittivities. *J Chem Phys* 1955; 23: 1514–1517.
127. Felderhof BU, Ford GW, Cohen EGD, et al. Cluster expansion for the dielectric constant of a polarizable suspension. *J Stat Phys* 1982; 28: 135–164.
128. Sen AK and Torquato S. Effective conductivity of anisotropic two-phase composite media. *Phys Rev B* 1989; 39: 4504–4515.
129. Torquato S. Exact expression for the effective elastic tensor of disordered composites. *Phys Rev Lett* 1997; 79: 681–684.
130. Torquato S. Predicting transport characteristics of hyperuniform porous media via rigorous microstructure-property relations. *Adv Water Resour* 2020; 140: 103565.
131. Klatt MA, Ziff RM, Torquato S, et al. Critical pore radius and transport properties of disordered hard-and overlapping-sphere models. *Phys Rev E* 2021; 104: 014127.
132. Torquato S. Diffusion spreadability as a probe of the microstructure of complex media across length scales. *Phys Rev E* 2021; 104: 054102.
133. Prager S. Diffusion and viscous flow in concentrated suspensions. *Physica* 1963; 29: 129–139.
134. Wang H and Torquato S. Dynamic measure of hyperuniformity and nonhyperuniformity in heterogeneous media via the diffusion spreadability. *Phys Rev Appl* 2022; 17: 034022.
135. Torquato S and Chen D. Multifunctionality of particulate composites via cross-property maps. *Phys Rev Mater* 2018; 2(9): 095603.
136. van der Linden JH, Narsilio GA, Tordesillas A, et al. Machine learning framework for analysis of transport through complex networks in porous, granular media: a focus on permeability. *Phys Rev E* 2016; 94: 022904.
137. Neumann M, Stenzel O, Willot F, et al. Quantifying the influence of microstructure on effective conductivity and permeability: virtual materials testing. *Int J Sol Struct* 2020; 184: 211–220.
138. Röding M, Ma Z, Torquato S, et al. Predicting permeability via statistical learning on higher-order microstructural information. *Scientific Rep* 2020; 10: 1–17.
139. Coker DA, Torquato S, Dunsmuir JH, et al. Morphology and physical properties of Fontainebleau sandstone via a tomographic analysis. *J Geophys Res* 1996; 101: 17497–17506.
140. Napadow VJ, Chen Q, Mai V, et al. Quantitative analysis of three-dimensional-resolved fiber architecture in heterogeneous skeletal muscle tissue using nmr and optical imaging methods. *Biophys J* 2001; 80: 2968–2975.
141. Blunt MJ, Bijeljic B, Dong H, et al. Pore-scale imaging and modelling. *Adv Water Resour* 2013; 51: 197–216.
142. Reid E, Buzzard GT, Drummy LF, et al. Multi-resolution data fusion for super resolution imaging. *IEEE Trans Comput Imaging* 2022; 8: 81–95.